RSC Sustainability

ROYAL SOCIETY OF CHEMISTRY

PAPER

View Article Online
View Journal | View Issue

Cite this: *RSC Sustainability*, 2025, **3**, 580

Task-specific ionic liquids and ultrasound irradiation: a successful strategy to drive the alcoholysis of polycarbonate†

Francesca D'Anna, *[a] Giovanna Raia,[a] Gianluca Di Cara,[b] Patrizia Cancemi [b] and Salvatore Marullo [a]

Received 12th June 2024
Accepted 20th December 2024

DOI: 10.1039/d4su00301b

rsc.li/rscsus

The release of plastics into the environment is a pressing issue of the modern society, and the identification of strategies for their recycling is a challenge in chemical research. This work analyses the possibility of combining the efficiency of task-specific ionic liquids (TSILs) with the effect of ultrasound irradiation (US) to perform the alcoholysis of polycarbonate (BPA-PC). Aliphatic cations were combined with environmentally friendly basic anions to obtain TSILs able to perform the process at room temperature. Different operational parameters were optimized. The process performance was evaluated using a holistic approach to green chemistry, and the best catalysts were tested for their cytotoxicity toward two different normal cell lines, namely, the mammary epithelium (HB2) and retinal pigment epithelium (hTERT-RPE-1) cell lines. The collected data demonstrated that the best catalyst performed the process at 30 °C with an irradiation time of 90 minutes, offering conversion and yield values higher than 80%. Interestingly, it could be used to process post-consumer samples, like a digital CD and a BPA-PC sheet, providing results comparable to the ones obtained using pristine BPA-PC and bisphenol A with good purity. Furthermore, the proposed protocol could be scaled up without a drop in performance.

Sustainability spotlight

Plastic waste diffusion in the environment harms both the ecosystem and human health. Plastic waste recycling represents a valuable strategy, especially considering the significant energy saving and constant pursuit toward a carbon-neutral society. Our interest was in designing plastic waste recycling processes that simultaneously offer high efficiency and low environmental impact. In this context, we proposed a combined approach based on the use of ultrasound irradiation and task-specific ionic liquids to perform the alcoholysis of polycarbonate. Interestingly, we achieved polycarbonate depolymerization at room temperature, using a robust protocol that could be easily scaled up and was based on catalysts showing very low cytotoxicity, thus adhering to SDG7, SDG9, and SDG13.

Introduction

Plastics and polymers heavily feature in the day-to-day life of the modern society. The use of plastic is spread across the fields of transportation, agriculture, communications as well as health-care. However, the use of plastics is designed for a limited time period, after which they become waste. Over the years, about 275 million metric tons of plastics waste were produced by 192 nations and a large amount of this, ranging from 4.8 to 12.7 million metric tons, was discharged in the oceans.[1]

Unfortunately, plastic waste does not disintegrate in water bodies, and it undergoes leaching, leading to the formation of micro- and nano-plastics. These small-sized plastics can release their additives, like toxic dyes, bisphenol A (BPA), phthalates, and so on, which are toxic both for animals and humans as they can mimic the function of some enzymes and hormones in the body, thus blocking biological functions.[2,3]

To deal with the above issue, most countries have imposed a partial or complete ban on certain plastics. However, considering the excellent properties and minimal cost of these materials, it is impossible to think about a life without them.

A valuable and more convenient approach is one that considers the safe and efficient disposal of plastic waste, also taking into consideration the possibility of their recycling. In this context, mechanical and chemical approaches could be used. Mechanical recycling is mainly used from an industrial point of view and involves material downcycling and repurposing its application to a lower value. In contrast, chemical

[a]*Università degli Studi di Palermo, Dipartimento STEBICEF, Sezione di Chimica, Viale delle Scienze, Ed. 17, 90128 Palermo, Italy. E-mail: francesca.danna@unipa.it*

[b]*Università degli Studi di Palermo, Dipartimento STEBICEF, Sezione di Biologia Cellulare, Viale delle Scienze, Ed. 16, 90128 Palermo, Italy*

† Electronic supplementary information (ESI) available: Tables summarizing the yield and conversion of reaction studied, NMR and IR spectra. See DOI: https://doi.org/10.1039/d4su00301b

recycling preserves the value of the product over many cycles. Its main purpose is to obtain the monomers involved in the plastic production, thereby inducing two main environmental benefits: (i) a decrease in plastic waste dispersion in the ecosystem and (ii) a significant reduction in the consumption of fossil fuels needed for the production of new plastic polymers.

Among the plastics that may undergo chemical recycling, polyesters have been largely investigated. In particular, different papers have focused on recycling processes for polyethylene terephthalate (PET) and polylactic acid (PLA),[4–7] due their widespread use, whereas polycarbonates (*e.g.*, poly(bisphenol A carbonate, BPA-PC) have been less explored.

BPA-PC shows many desirable properties, and is widely used as a thermoplastic polymer due to its good stability and rigidity, transparency, excellent flame redundancy, and high impact resistance.[8] It is currently used for containers and automobile parts, in health care applications, as digital storage media, and electronic casing, and so on. This explains why its production has gradually increased up to 5 tons per year.[9] However, the environmental impact of BPA-PC represents a pressing issue as its degradation in the environment causes the release of BPA, which is harmful to human health. Indeed, it can behave as an estrogen-like agent in the human body, inducing hormone disrupting effects.[10]

All the above considerations explain why the recycling of plastics waste and, especially BPA-PC, is becoming mandatory.

A deep survey of the literature demonstrates how, so far, different approaches have been used for BPA-PC recycling.[11,12] These methods include methanolysis,[13–16] glycolysis, and aminolysis.[17,18] All these methods offer the advantage of recovering BPA, but also allow producing certain chemical intermediates that are normally obtained using harsh conditions and harmful reagents.

Focusing on alcoholysis, beside BPA recovery, this kind of recycling approach also allows obtaining important chemical intermediates, like alkyl carbonates. These are normally obtained by reacting dichlorocarbonate in the presence of a large amount of alcohols. Dialkylcarbonates are industrially relevant as replacements for hazardous chemical reagents or reactive solvents, but they also find application in lubricants, cosmetics, fuels, and pharmaceutical compositions.[19–21] Consequently, the alcoholysis of discharged BPA-PC could represent a valuable strategy for achieving not only zero waste but could also offer the possibility to decrease the impact of some other industrially relevant processes. This explains the surge of interest that, since 1998, the scientific community has devoted to this topic. Different methods have been reported that foresee the use of different catalysts, like alkali[22] mesoporous molecular sieves,[23] organocatalysts,[24] and supported alkaline earth metal oxides.[16,25,26] Furthermore, recently, also the use of non-conventional solvents, like ionic liquids and deep eutectic solvents, has also been considered in the optimization of such kinds of processes.[27–31]

In this context, we recently explored the possibility of using task-specific ionic liquids (TSILs) in the recycling of polyesters, like poly(ethyleneterephtalate) and polycarbonate (BPA-PC).[32,33] In particular, the main aim of the work performed was to attempt optimization of the reaction conditions to maximize waste recycling by using environmentally friendly catalysts and minimizing energy demand. To pursue the above aims, in the case of BPA-PC, we combined the efficiency of TSILs with ultrasound (US) irradiation. Recently, there has been increasing interest in industrial applications of US, mainly because of the significant reduction in energy waste and improvement in processes performance that such a kind of methodology enables.[34–36] In our case, it could facilitate sustainable and green plastics recycling when considering various aspects, such as operational costs and energy intensity,[37–39] in which the nature and efficiency of the catalysts could play a pivotal role.

The approach used allowed us to obtain good conversion and yield values under very mild reaction conditions.[33] Furthermore, careful analysis of the effects derived from the different catalysts' structures allowed identifying features that act as key factors in the target process outcome. The screening of different anions allowed assessing the high efficiency of imidazolate-based catalysts. On the other hand, using the same anions, the comparison between cholinium- and ammonium-based ILs demonstrated the pivotal role played by the hydroxyethyl chain on the cation structure in promoting the alcoholysis of BPA-PC.[33]

With the above results in mind and with the aim to design eco-sustainable processes to perform the alcoholysis of BPA-PC, in the present study we initially took in to consideration the use of some imidazolate-based TSILs with differing cation structures (Scheme 1).

In particular, considering the relevance of the hydrogen bond donor ability of the IL cation in favoring nucleophilic addition to the carbonyl group of the ester function,[33] we prepared tetramethylguanidinium ([TMG^+]), hydroxyethylmethylpyrrolidinium ([$C_1C_2OHPyrr^+$]), hydroxyethylmethylpiperidinium ([C_1C_2-$OHPip^+$]), hydroxyethylmethylmorpholinium ([$C_1C_2OHMor^+$]), and 1,4-diazabicyclo-[2.2.2]-octane-based ([$(C_2OH)_2DABCO^{2+}$]) ILs. This set could help to verify if a different nature of the cationic head would affect the performance of the process, mainly using aliphatic cations that are well known for their lower toxicity with respect to the corresponding aromatic ones.[40] Furthermore, ionic liquid-based catalysts were used for their well-known low corrosivity, which could represent a significant advantage for large-scale application.

Catalytic tests were performed at 30 °C under US irradiation, analyzing the effect of the reaction time and temperature, and also catalysts derived from different ratios between the moles of catalyst and the number of repeating units in the polymer (n_c/n_{RU}). Moreover, for the best cationic moiety, different anions, such as phosphate, succinamidate, and amino acid ones, were tested, as well as different nucleophiles to gain insights into the role played by steric hindrance on the performance of the process and to assess the possibility to obtain alkyl carbonates with different natures. The most efficient catalysts were also used for the methanolysis of real samples, like a polycarbonate sheet and a digital support (CD). We also performed scale up of the process using a five times larger amount of BPA-PC.

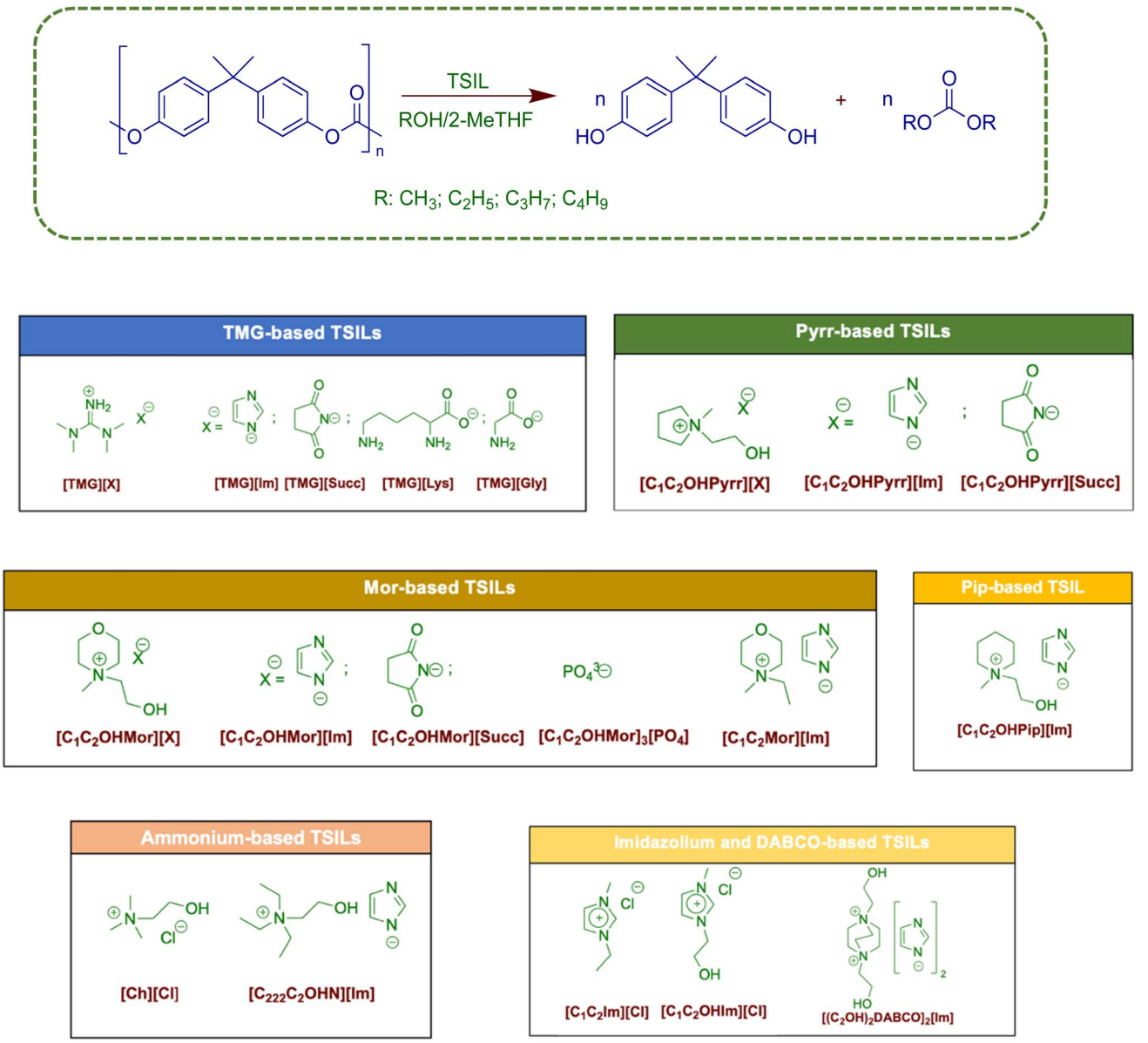

Scheme 1 Reactions that were studied and structures of the catalysts.

Obviously, in performing such kinds of processes, also the toxicity and environmental impact of the catalysts must be evaluated. For this reason, the best performing catalytic systems were tested for their toxicity toward mammary and retinal pigment epithelium normal cell lines, like HB2 and hTERT-RPE-1.

The data collected demonstrated that properly designing the structure of TSILs and combining them with US irradiation could facilitate eco-sustainable processes for the methanolysis of BPA-PC, not only in terms of efficiency and energy demand, as demonstrated by their evaluation using the holistic approach to green chemistry,[41] but also in terms of safety and post-process discharge. To the best of our knowledge, this is the first report in which plastic waste recycling, performed using IL-based catalysts, has considered the toxicity aspects related to the catalyst structure.

Results and discussion

Preliminary catalytic tests

Preliminary catalytic tests were carried out taking in to consideration the data previously collected for the methanolysis of BPA-PC using cholinium-based TSILs under US irradiation.[33] The information previously gained shed light on the high catalytic activity of **[Ch][Im]**, which combined the high basicity of the anion with the ability of the hydroxylethyl chain on the cation to coordinate the carbonyl group of BPA-PC, increasing its electrophilicity. Interestingly, as previously reported, this action was activated only under US irradiation, as the target process did not occur at room temperature or under silent conditions.[33]

On the grounds of the above information, the first catalytic run was performed using **[TMG][Im]**, chosen for the well-known

proton-donor ability of the [TMG$^+$] cation.[42,43] The target process was carried out using the previously determined reaction conditions,[33] working at 30 °C and using a mass ratio of 2-MeTHF/MeOH equal to 3 and an n_c/n_{RU} ratio equal to 1/12 (where n_c represent the moles of the catalyst and n_{RU} the number of moles of repeating units in the polymer), increasing the irradiation time from 105 up to 135 min (Table S1†).

It is noteworthy that the use of 2-MeTHF, as a swelling agent, rather than the normally used THF, was due to the possibility of using a solvent that could be obtained from biomass rather than fossil fuels.[44] Furthermore, our previous results[33] demonstrated that using this solvent, rather than THF, did not significantly affect polymer swelling, as the performance of the process stayed practically unchanged. Analysis of the conversion and yield values demonstrated that the increase in reaction time induced a parallel increase in conversion, which changed from 72% up to 84%. Interestingly, the use of a larger irradiation time also caused a significant increase in selectivity, as accounted for by the yields, which changed from 57% up to 81%. Probably, a longer US irradiation favors oligomers breakdown, increasing the amount of BPA recovered. Notably, when going from 120 up to 135 min, no significant changes in both the yield and conversion values were obtained, so allowing the identification of the shorter one as the best condition in terms of energy saving.

TSIL cation effect

With the above results in mind, we analyzed the effect derived from the different natures of the cationic head, taking in to consideration *N*-hydroxyethyl-based cations. In particular, under the best experimental conditions, we tested the efficiency of **[C_1C_2OHPyrr][Im]**, **[C_1C_2OHPip][Im]**, **[C_1C_2OHMor][Im]**, and **[$(C_1C_2OH)_2$DABCO][Im]$_2$**. In all cases, we used aliphatic cations and we tried to mitigate their toxicity with the presence of the hydroxylated side chain and, in the case of morpholinium-based ILs, also with the presence of oxygen in the heterocyclic ring structure. The conversion and yield values are displayed in Fig. 1 (Table S2†). For a useful comparison, data previously obtained using **[Ch][Im]** are also reported.[33]

The data collected show that the performance of the process was significantly affected by the cation structure. Indeed, the conversions ranged from 59% up to 86%, while the yields changed from 52% up to 82%. With the only exception of **[C_1-C_2OHPip][Im]**, in all the other cases small differences between the conversion and yield values were detected, indicating a very high selectivity for the target process.

Among the tested TSILs, **[$(C_2OH)_2$DABCO][Im]$_2$** proved to be the least efficient, with conversion values lower than 60%. Probably this is a consequence of its low solubility in the solvent media, whereas **[TMG][Im]** and **[C_1C_2OHMor][Im]** gave rise to the highest conversion and yield values. In general, the yields changed along the order: **[C_1C_2OHPip][Im]** < **[C_1C_2OHPyrr][Im]** < **[$C_{222}C_2$OHN][Im]** < **[TMG][Im]** < **[C_1C_2OHMor][Im]**. Then, among the cyclic cations, piperidinium and pyrrolidinium were less efficient than the morpholinium one in favoring BPA-PC conversion. In particular, as accounted for by the lower selectivity, with respect to the other cyclic cations, the piperidinum one was less able to favor oligomers breakdown and BPA formation. On the other hand, comparison between the data collected for **[C_1C_2OHPip][Im]** and **[C_1C_2OHMor][Im]** evidenced a positive effect derived from the presence of oxygen in the heterocyclic ring.

TSIL anion effect

With the above information in mind, we tried to analyze the anion effect, considering **[TMG$^+$]**-, **[C_1C_2OHPyrr$^+$]**-, and **[C_1C_2-OHMor$^+$]**-based catalysts, on the grounds of their good performance detected. We used anions with low environmental impact, like the ones derived from the amino acids glycine and lysine, succinimidate, together with imidazolate and phosphate on the grounds of their previously detected catalytic ability toward the target process.[33] The data collected are reported in Fig. 2 and Table S3.†

Analysis of the data collected evidenced the moderate catalytic ability of the **[Succ$^-$]**-based catalysts. Differently, the catalytic activity increased going to **[PO_4^{3-}]**-based ILs, with the highest conversion and yield values obtained in the presence of **[Im$^-$]** anions. In the case of **[TMG$^+$]**-based catalysts, the worst results were collected by using amino acid-based TSILs. However, these were the only catalysts that did not dissolve completely in the reaction mixture.

To rationalize the above results, we first evaluated the basicity of the TSILs, determining the Hammett basicity

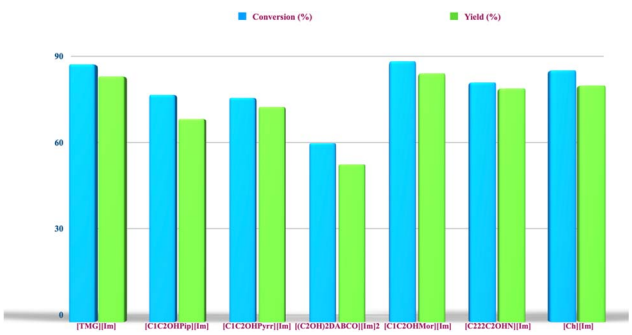

Fig. 1 Conversion and yield values for the methanolysis of BPA-PC, under US irradiation (50 W, 250 kHz) at 30 °C for 120 minutes, as a function of the nature of different catalysts (n_c/n_{RU} = 1/12; $m_{2\text{-MeTHF}}/m_{MeOH}$ = 3). Conversion and yield values were reproducible within ±3%. Values for [Ch][Im] are taken from ref. 33.

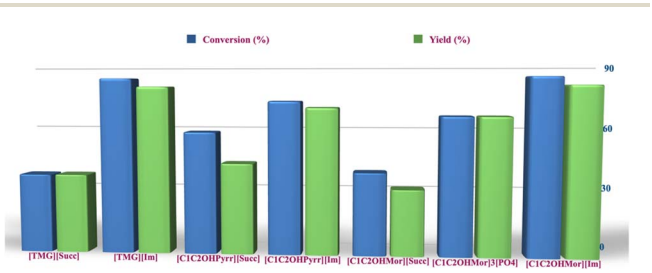

Fig. 2 Conversion and yield values for the methanolysis of BPA-PC, under US irradiation (50 W, 250 kHz) at 30 °C for 120 minutes, as a function of the nature of different catalysts (n_c/n_{RU} = 1/12; $m_{2\text{-MeTHF}}/m_{MeOH}$ = 3). Conversion and yield values were reproducible within ±3%.

function (H_-), using *p*-nitrophenol as a spectroscopic probe. We previously used this procedure to determine amine basicity in IL solutions,[45,46] but also to determine the basicity of some TSILs used as catalysts to promote the mononuclear rearrangement of heterocycles[47] and the Michael addition.[48] The data collected are displayed in Table S4.†

Comparison among the H_- values and the conversion and yield values demonstrated that the TSILs basicity could explain the observed trends only if the cation structure stayed constant. Indeed, with the only exception of **[TMG][Succ]**, the conversion and yield increased, according to H_- value, always giving the highest values for the [Im]-based catalyst. On the other hand, in the case of the [$C_1C_2OHMor^+$]-based catalysts, the catalytic ability perfectly fitted the basicity trend.

Surprisingly, for **[TMG][Lys]** and **[TMG][Gly]**, we measured H_- values ranging from 10.5 up to 10.8, comparable to the ones collected for **[$C_1C_2OHMor]_3[PO_4]$** or **[C_1C_2OHMor][Im]**, supporting the hypothesis that the low catalytic ability of the above TSILs could not be ascribed to a low basicity but rather to their low solubility in the reaction media.

Optimization of the experimental conditions

Having identified the best catalysts, we analyzed the effect of different operational parameters, like the irradiation time, the n_c/n_{RU} ratio, the mass ratio between 2-Me-THF and methanol, and the temperature effect.

In all cases, **[C_1C_2OHMor][Im]** was used as the catalyst. Only in the case of the evaluation of the irradiation time, a **[TMG][Im]** was also tested. The data relevant to this latter evaluation are reported in Fig. 3 and Table S5.†

Analysis of the data reported in Fig. 3 evidenced the different behaviors of the tested catalysts. Indeed, in the case of **[TMG][Im]**, going from 105 up to 135 min, significant increases in conversion, yield, and selectivity were detected.

Differently, as far as **[C_1C_2Mor][Im]** was concerned, a significant improvement in catalyst performance was detected at 90 min. The above results testify the high efficiency of the latter catalyst, which was able to give conversion and yield values comparable to the ones collected in the presence of **[TMG][Im]**, but in a significantly lower reaction time. This is the reason why it was used in all the other optimization tests.

According to green chemistry principles, the design of new chemical processes should take in to consideration the possibility of minimizing the amount of materials and energy used. In light of the above considerations, we assessed the effects derived from the n_c/n_{RU} ratio, the amount of swelling agent, and the temperature effect. The data collected are reported in Tables S6–S8.† Analysis of the collected results indicated an n_c/n_{ru} ratio equal to 1/12 was the best catalyst loading (Table S6†). Indeed, the conversion and yield gradually increased, going from 1/6 up to 1/12, but stay constant with further decreasing the above parameter. This result perfectly agreed with the one we previously collected performing the same process in the presence of cholinium-based catalysts.[33]

As for the amount of the swelling agent, we changed the mass ratio between 2-MeTHF and MeOH from 5/3 up to 7/1 (Table S7†). The results collected indicated a gradual increase in both the conversion and yield values going from 5/3 up to 6/2, but the further increase in the amount of 2-MeTHF induced a significant decrease in the above parameters. The above results could be explained considering the role played by both the nucleophile and the swelling agent. Probably, a 6/2 mass ratio represents the best compromise between the extent of swelling of the polymeric structure that would make available the ester carbonyl group, and the amount of the nucleophile, which is essential to favor the ester group breakdown.

Finally, we also investigated the effect of the temperature, carrying out the process in the range of 20–40 °C (Table S8†). Interestingly, a significant increase in conversion and yield was detected going from 20 °C up to 30 °C. However, the further rise in temperature to 40 °C decreased the above parameters together with the selectivity of the process.

Mechanistic hypothesis

Analysis of the results collected using **[C_1C_2OHMor][Im]** as the catalyst immediately sheds light on the better performance of

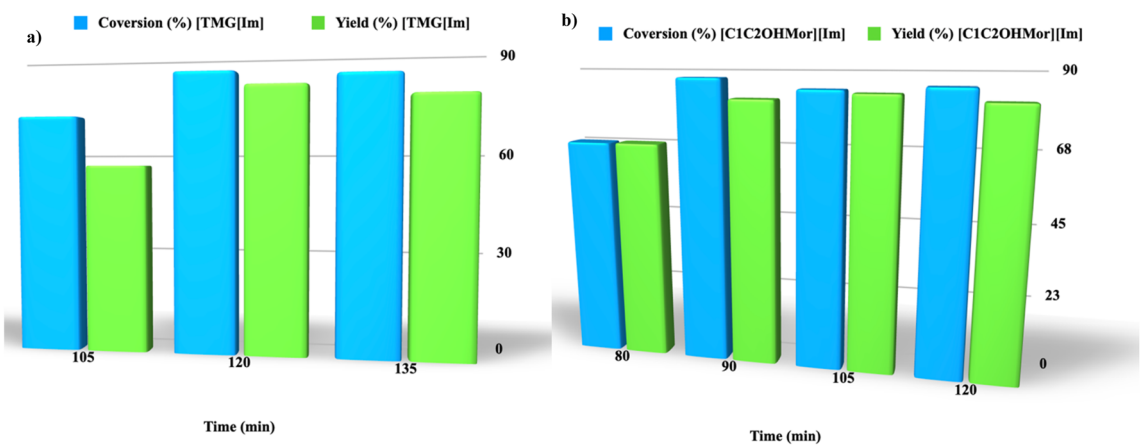

Fig. 3 Conversion and yield values for the methanolysis of BPA-PC, under US irradiation (50 W, 250 kHz) at 30 °C, as a function of time: (a) in the presence of [TMG][Im]; (b) in the presence of [C_1C_2OHMor][Im] (n_c/n_{RU} = 1/12; $m_{2\text{-MeTHF}}/m_{MeOH}$ = 3). Conversion and yield values were reproducible within ±3%.

this TSIL with respect to the previously reported **[Ch][Im]**.[33] Indeed, with the reaction temperature and n_c/n_{ru} being the same, this catalyst was able to give comparable conversion and yield values, but in a lower reaction time (105 and 90 min for **[Ch][Im]** and **[C_1C_2OHMor][Im]**, respectively). This, according to green chemistry principles, will enable significant energy saving.

On the grounds of the above information and with the aim to explain the above catalytic effect, we first attempted the synthesis of **[C_1C_2OHIm][Im]** and **[C_1C_2Im][Im]** to assess the possible role played by both the hydrogen donor ability of C2–H on the imidazolium ring[49] and the OH group on the side chain. Unfortunately, the basicity of [Im$^-$] anion was able to induce the breakdown of the C2–H bond on the imidazolium ring, favoring carbene formation. This is the reason why we tested, under the best experimental conditions, the performance of the corresponding chlorides, **[C_1C_2OHIm][Cl]** and **[C_1C_2Im][Cl]**. The results collected are reported in Fig. 4 and Table S9.†

Analysis of collected results confirmed the relevance of the role played by the hydroxyl side chain. Indeed, notwithstanding the well-known acidity of the C2–H bond of the imidazolium ion,[50] no BPA-PC conversion was observed in the presence of **[C_1C_2Im]Cl**. Differently, the use of **[C_1C_2OHIm]Cl** allowed obtaining conversion and yield values higher than 60%. Surprisingly, the effect of the hydroxyl side chain proved to be less relevant when **[C_1C_2Mor][Im]** was used as the catalyst (Fig. 4 and Table S9†). Indeed, in this case, only small changes in conversion and yield were detected with respect to **[C_1C_2OHMor][Im]**. To explain the above result and to rationalize the higher process rate with respect to the previously used **[Ch][Im]**, we supposed that **[C_1C_2OHMor][Im]** could behave as a trifunctional catalyst, in which beside the increase in electrophilicity of the carbonyl group induced by the hydroxyl side chain, the process was assisted by a significant rise in the alcohol nucleophilicity due to the coordination of the alcoholic proton by both the [Im$^-$] anion and heterocyclic oxygen atom of the morpholinium cation (Scheme 2).

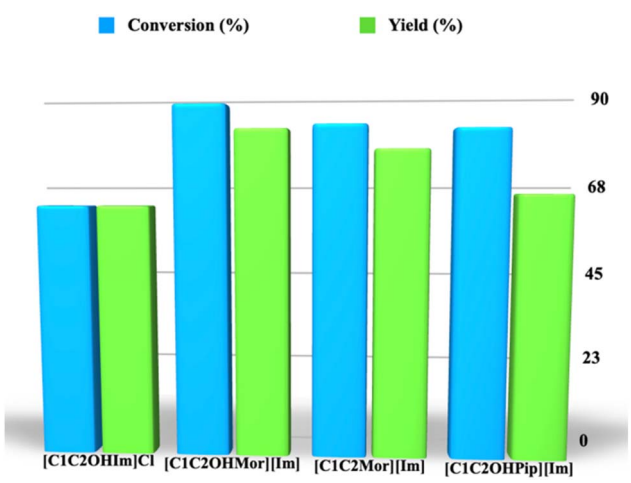

Fig. 4 Conversion and yield values for the methanolysis of BPA-PC, under US irradiation (50 W, 250 kHz) at 30 °C, in the presence of different catalysts (n_c/n_{RU} = 1/12; $m_{2\text{-MeTHF}}/m_{MeOH}$ = 3). Conversion and yield values were reproducible within ±3%.

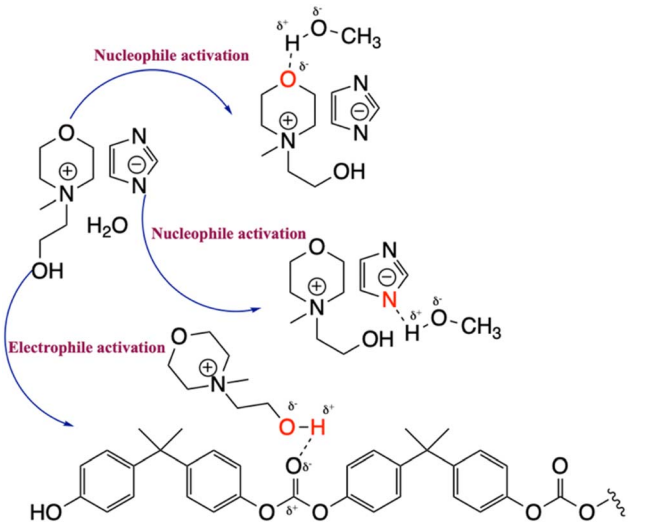

Scheme 2 Mechanistic hypothesis for BPA-PC breakdown in the presence of [C_1C_2OHMor][Im].

To verify the above hypothesis, we carried out the methanolysis of BPA-PC using **[C_1C_2OHPip][Im]**, *i.e.*, lacking the heterocyclic oxygen. We observed a small decrease in conversion (88% and 80% in the presence of **[C_1C_2OHMor][Im]** and **[C_1C_2OHPip][Im]**, respectively), probably indicating a comparable ability of the catalysts to favor oligomers formation, but a significant lower efficiency of **[C_1C_2OHPip][Im]** in inducing their breakdown, favored by the presence of a higher nucleophile concentration.

To further support this hypothesis, we recorded the ^{1}H NMR spectra of **[C_1C_2OHMor][Im]** and **[C_1C_2OHPip][Im]** in the presence of methanol, to gain insights into the possible interactions between the catalysts and alcohol (Fig. S1 and Table S10†). Comparison between the spectra in the presence and in the absence of methanol, with the same catalyst, showed there was a downfield shift of the signals corresponding to the imidazolate anion. Interestingly, the above shift proved to be more relevant for the H2 proton of the heterocyclic ring and was larger in the case of **[C_1C_2OHPip][Im]** ($\Delta\delta$ = 0.22 ppm) than in the case of **[C_1C_2OHMor][Im]** ($\Delta\delta$ = 0.1 ppm).

The above result sheds light on the different involvement of the imidazolate anion in the interaction with the alcohol. In particular, in the case of the morpholinium-based catalyst, the heterocyclic oxygen atom of the ring probably shares the role of a hydrogen bond acceptor site with the anion, indicating a lower involvement of this latter in the interaction with the alcohol and explaining the lower change in the chemical shift value. The same factor could explain the comparable performance of **[TMG][Im]** and **[C_1C_2OHMor][Im]**, notwithstanding the significantly higher hydrogen bond donor ability of the former. Probably, the contribution of the heterocyclic oxygen atom, in coordinating the hydroxyl proton, partially compensated for the lower ability of the **[C_1C_2OHMor$^+$]** cation to increase the electrophilicity of the carbonyl group, giving rise to comparable

conversion and yield values. We are aware of the fact that also the [Im^-] anion could behave as a nucleophile toward the carbonyl group. However, we rejected this possibility on the grounds of both the large excess of alcohol in the solvent media and its lower steric hindrance with respect to the [Im^-] anion.

Nucleophile effect

In light of the above information and with the best reaction conditions in hand, we performed the process but with changing the nature of the nucleophile and testing ethanol, propanol, butanol, and ethylene glycol. This kind of investigation could allow gaining information about the effect derived from a gradual increase in the steric hindrance of the nucleophile because of the alkyl chain lengthening, On the other hand, it also has further relevance from an environmental point of view, as beside BPA, changing the nature of the alcohol could allow the obtainment of alkyl carbonates with different natures, which would be of industrial relevance, as they are frequently used as benign alternatives to conventional organic solvents and applied in different sectors, like automotive, and health care.[51] Over the years, different synthetic procedures have been suggested for alkyl carbonates preparation.[51] However, the most widely used is the one with phosgene as a reagent, which is well known for its cytotoxicity and environmental impact.[52]

Consequently, the obtainment of dialkylcarbonates as products of BPA-PC recycling offers the advantage of improving the sustainability of a chemical process while also enabling the full recovery of a waste material. The data collected as a function of the different nature of the nucleophile are reported in Fig. 5 and Table S11.†

The conversion and yield values gradually decreased going from methanol to ethylene glycol, according to the increase in the alkyl chain length of the alcohol and its steric hindrance. However, in the case of ethylene glycol, the collected result could be also ascribed to the lower solubility of the alcohol in the mixture.

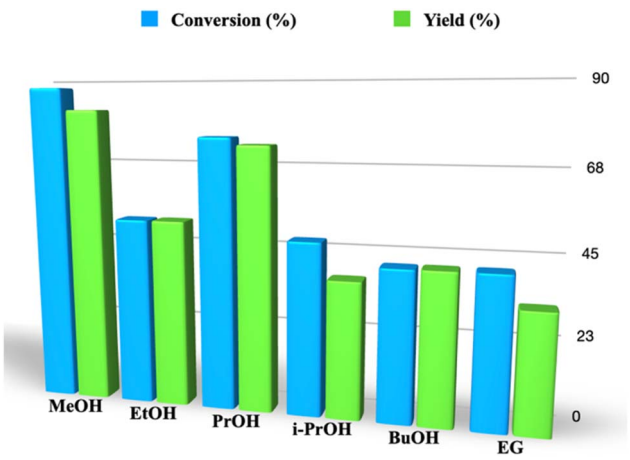

Fig. 5 Conversion and yield values for the alcoholysis of BPA-PC, under US irradiation (50 W, 250 kHz) at 30 °C, in the presence of different nucleophiles (n_c/n_{RU} = 1/12; $m_{2\text{-MeTHF}}/m_{MeOH}$ = 3). Conversion and yield values were reproducible within ±3%.

Another key factor in determining the obtained trend could also be the alcohol viscosity. Indeed, the conversion and yield values decreased in good agreement with the alcohol viscosity (η = 0.55, 1.09, 1.95, 2.53, 2.86, and 21 mPa s for MeOH, EtOH, PrOH, i-PrOH, BuOH, and EG), even though differences in the above parameter did not always account for the differences detected. To this aim, it is important to consider that an increase in solvent viscosity generally disfavors the formation of cavitation bubbles. However, the resulting ones proved to be more energetic, inducing a major effect on the outcome of the reaction. Consequently, the observed trend could be the result of a balance of the above contrasting factors.

Evaluation of the process and cytotoxicity of the best catalysts

As a further attempt to assess the sustainability of our protocol, we applied the holistic approach to green chemistry,[41] at a laboratory scale. It was noteworthy that this approach aims for a critical analysis of a chemical process, using a toolkit, to evaluate the state of art of a given process and critical points in the used methodologies with the aim to improve it. On a laboratory scale, at the zero level, evaluation parameters like the conversion, yield, and selectivity are used, that gain sustainability indicators of different colors, as a function of their values (green > 89%, yellow 70–89% and red < 70%). The results collected, using different catalysts, are reported in Table S12.† Analysis of the data collected allowed identifying **[TMG][Im]**, **[$C_{222}C_2OHN$][Im]**, and **[C_1C_2OHMor][Im]** as the best catalysts. They all showed green indicator for selectivity and yellow indicators for conversion and yield.

With the above information in mind and according to the green chemistry principles for avoiding the use of toxic reagents, the best catalysts identified on the ground of the holistic approach were tested toward two different normal cell lines, namely HB2 and hTERT-RPE-1 of mammary and retinal pigment epithelial cells, respectively. Interestingly, in both cell lines, no morphological change or cell number reduction was detected, after 24 h of treatment with 1.6 mM of **[TMG][Im]**, **[$C_{222}C_2OHN$][Im]**, and **[C_1C_2OHMor][Im]**, compared to control cells. In fact, the treated cells displayed a similar morphology to the untreated ones, as reported in Fig. 6.

Toxicity tests were carried out after 48 h of treatment using the MTT assay and the results collected are reported in Fig. 7. The IC_{50} values are displayed in Table S13.†

Analysis of the collected data evidenced the ability of the tested catalysts to exert toxicity effects only at a very high concentration, and after 48 h of treatment, highlighting their significantly low cytotoxicity. The IC_{50} values obtained from the dose–response curves were always in the mM range, and proved to be affected by the cation structure (Table S13†). Indeed, independently from the cell line nature, they decreased going from **[TMG][Im]** to **[C_1C_2OHMor][Im]** and **[$C_{222}C_2OH$][Im]**.

Recycling of the catalysts, post-consumer samples treatment, and scale up

With the aim to decrease the amount of waste obtained from the process, we attempted catalyst recycling. To this aim, two of

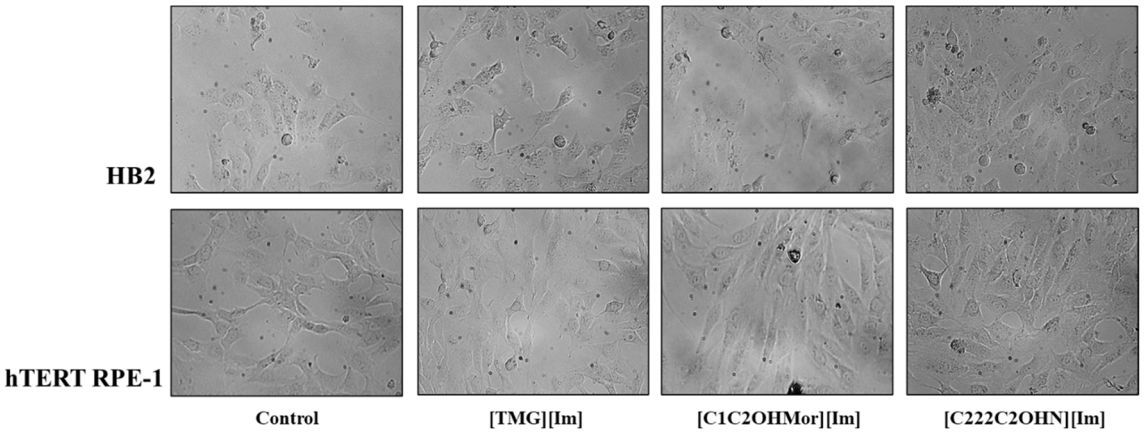

Fig. 6 Inverted phase-contrast micrographs of HB2 and hTERT RPE-1 normal epithelial cells treated for 24 h with 1.6 mM of [TMG][Im], [$C_{222}C_2$OHN][Im], and [C_1C_2OHMor][Im]. Magnification 200×.

the best catalysts, namely **[TMG][Im]** and **[C_1C_2OHMor][Im]**, were recovered after the first cycle by evaporating the aqueous solution under pressure, and were then reused. Unfortunately, in both cases, they proved to be inactive. With the aim to understand the above result, **[C_1C_2OHMor][Im]** was irradiated under the best experimental conditions, but in the absence of the polymer. Surprisingly, the ^{1}H NMR spectra of the recovered catalyst showed the presence of some additional peaks, which could be confidently ascribed to partial catalyst degradation (Fig. S2†).

In setting such kind of processes, the applicability of the protocol to post-consumer samples is quite important. Indeed, the presence of additives derived from polymer manufacturing might compromise the performance of the recycling process. To this aim, under the best reaction conditions and using **[C_1C_2OHMor][Im]**, we carried out the methanolysis of a digital CD and a BPA-PC sheet. The data collected are reported in Fig. 8 and Table S14† and verified the overall applicability of our protocol.

Indeed, in both cases, the conversion and yield values were comparable to the ones we detected using commercial BPA-PC grains. On the other hand, to check the purity of the BPA obtained, we recorded its ^{1}H NMR, ^{13}C NMR, and IR spectra, and found no evidence of the presence of any by-products. This demonstrates the possibility to obtain BPA with good purity also from real samples (Fig. S3†).

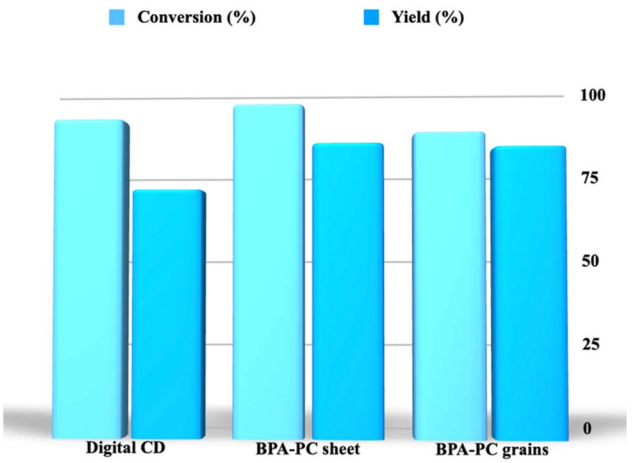

Fig. 8 Conversion and yield values collected for the methanolysis of a digital CD, BPA-PC sheet, and BPA-PC grains, using [C_1C_2OHMor][Im] (n_c/n_{RU} = 1/12; $m_{2\text{-MeTHF}}/m_{MeOH}$ = 3) as the catalyst, under US irradiation (50 W, 250 kHz) at 30 °C for 90 min. Conversion and yield values were reproducible within ±3%.

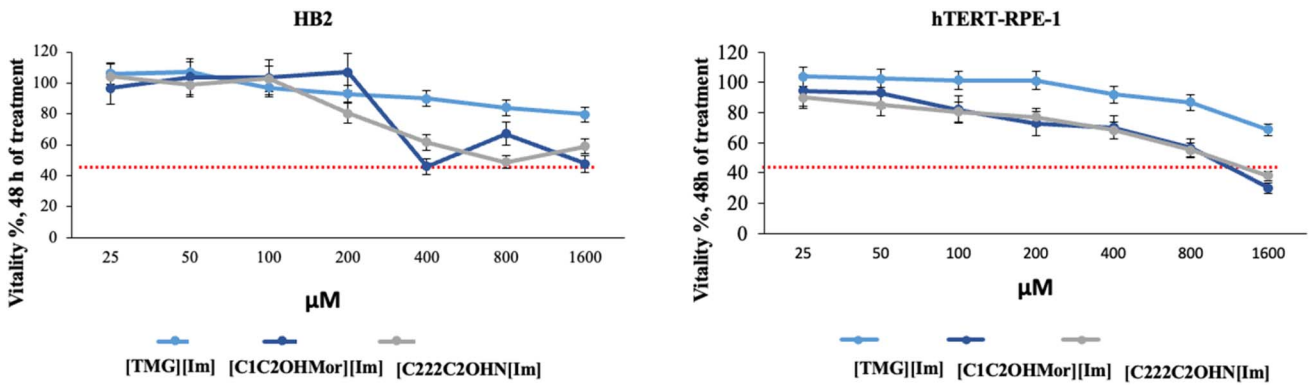

Fig. 7 Plots of the cell viability as a function of catalyst concentration for HB2 and hTERT RPE-1.

Table 1 Comparison between the yield and conversion values obtained in this work for the methanolysis of BPA-PC and with the ones previously reported in the literature

Entry	Catalyst	Conversion (%)	Yield (%)	T (°C)	t (min)	Reference
1	$[C_1C_2OHMor][Im]$	86	82	30 (US)	90	This work
2	[Ch][Im]	83	38	30 (US)	105	33
3	[bmim][OAc]	100	95	90	150	31
4	[bmim]Cl	100	95	105	150	31
5	NaOH	62	52	30 (US)	90	This work
6	NaOH	100	96	70	60	22
7	NaOH	100	94	100	480	53
8	NaOH	100	90	30 (US)	45	54
9	Ce_2O–CaO–ZrO_2	100	—	100	120	26
10	ChCl/U (1 : 2)	100	99	130	150	55
11	[HDBU][Suc]	100	96	70	120	29
12	Mg/Al layered double hydroxides	100	98	110	60	16
13	[EmimOH]Cl/U (1 : 2)	100	98	120	120	16

Finally, we also evaluated the possibility to apply the protocol to a larger amount of polymer, processing 10 g of polymer, under the best experimental conditions, and obtained conversion and yield values equal to 97%.

Comparison with the literature

To assess the relevance of the collected data, a comparison with the results previously reported in the literature was mandatory. To this aim, in Table 1 data relevant to methanolysis of BPA-PC performed using catalysts with different natures, under heating and under US irradiation, are reported.

Analysis of the data reported in Table 1 evidences that one of the most efficient catalysts reported in the literature is NaOH. To compare the performance of our best catalyst, $[C_1C_2OHMor][Im]$, with the one of sodium hydroxide, we carried out the methanolysis of PC under our best experimental conditions (T = 30 °C; t = 90 min; n_c/n_{RU} = 1/12), obtaining conversion and yield values lower than the ones collected using TSIL (entries 1 and 5). Taking in to consideration the lack of recyclability of our catalyst, we evaluated the environmental factor (E) under the worse scenario (no recyclability of the catalyst or solvents), obtaining a lower value when $[C_1C_2OHMor][Im]$ was used (E = 6.0 and 10.0 kg kg^{-1} for $[C_1C_2OHMor][Im]$ and NaOH, respectively).

Furthermore, a deep examination of the whole data reported in Table 1 immediately sheds light on the advantages of using our experimental protocol in terms of the reaction time and temperature. Indeed, with the only exception of the US-activated process performed using NaOH (entry 7) or **[Ch][Im]** (entry 2) catalysts that used a comparable temperature, in all other cases, the temperature ranged from 60 °C up to 120 °C. On the other hand, the above-mentioned cases were also the ones in which the reaction times were slightly longer (105 min, entry 2) or significantly shorter (45 min, entry 8). However, in the last case, a highly corrosive depolymerizing agent was used in a higher amount (n_c/n_{RU} = 1/7.6).

In general, the conversion and yield values collected in this work proved comparable to the ones previously collected by us using cholinium-based TSILs, or slightly lower than the ones so far reported and generally accounting for a total conversion of BPA-PC. However, as previously claimed, the suggested protocol shows the advantage of using safe catalysts that can be applied with very good results also to real samples and large amounts of plastic polymers.

Conclusions

With the aim to identify a strategy to perform the chemical recycling of BPA-PC, in this work, we combined the performance of TSILs and US irradiation to carry out the alcoholysis of the above polyester. TSILs were properly designed in an attempt to gain both catalytic efficiency and low toxicity, joining the properties of some *N*-hydroxyethyl-based aliphatic cations with those of basic environmentally friendly anions. These catalysts were used as potential substitutes for alkaline hydroxides, with the main benefit derived from their low corrosivity. Optimization of the experimental conditions demonstrated that the target process could be carried out with excellent results at 30 °C using an irradiation time equal to 90 min and a low catalyst loading. A deep analysis of the structural parameters affecting the performance of the catalysts indicated that the best one, namely **$[C_1C_2OHMor][Im]$**, behaved as a trifunctional catalyst, being able to increase the alcohol nucleophilicity through the anion and oxygen of the heterocyclic ring and the ester group electrophilicity by the intervention of the *N*-hydroxyethyl function.

The performances of all the tested catalysts were evaluated using a holistic approach based on green chemistry principles, at the zero level,[41] identifying the best catalysts either from the environmental point of view or the cytotoxicity aspect, when tested toward two different epithelial cell lines. To the best of our knowledge, this is the first report about PC recycling, taking in to consideration not only the performance, but also the possible impact of the catalyst used at the end of the process.

Interestingly, the data collected showed that the optimized protocol could be successfully applied to post-consumer samples, like a digital CD and a BPA-PC sheet, and could be

scaled up without a loss of performance. The results collected using the best performing catalyst proved comparable to the ones so far reported in the literature, but with a significant advantage in terms of a lower catalyst loading and toxicity as well as shorter reaction time and lower temperature.

On the whole, the proposed recycling strategy represents a robust protocol that can significantly contribute to boosting the chemical recycling of plastic polymers.

Experimental section

Materials

1,1,3,3-Tetramethylguanidine, *N*-methylpyrrolidine, *N*-methylpiperidine, *N*-methylmorpholine, 1-methylimidazole, triethylamine, imidazole, succinimide, L-lysine, glycine, 2-bromoethanol, iodoethane, phosphoric acid, 1-ethyl-3-methylimidazolium bromide, hydrochloric acid, and Amberlite 400-IRA chloride-form were purchased and used without further purification. Commercially available bisphenol A polycarbonate (Aldrich, pellet, 3 mm nominal granule size; Mw ~45 000 by GPC), PC sheets (thickness 3 mm, size 220 × 300 mm), 2-methyltetrahydrofuran, methanol, ethyl acetate, and sodium hydroxide were used without further purification.

1,1,3,3-Tetramethylguanidinium imidazolate ([TMG][Im]) and 1,1,3,3-tetramethylguanidinium succinimidate ([TMG][Succ]) were synthesized following procedures reported in the literature.[56,57]

General procedure for the synthesis of [TMG][Lys] and [TMG][Gly]

The amino acid (0.017 mol) was dissolved in 5 mL of water and to this solution a stoichiometric amount of 1,1,3,3-tetramethylguanidine was slowly added under stirring. The resulting mixture was kept at 40 °C for 24 h. Subsequently, the solvent was removed by evaporation at reduced pressure.

General procedure for the synthesis of piperidinium-, pyrrolidinium-, ammomium-, imidazolium-, and morpholinium-*N*,*N*-(2-hydroxyethyl)1,4-diazabicyclo[2.2.2]octane-based halide salts

Halide salts were synthesized following a procedure reported in the literature.[58] In particular, the suitable amine (2×10^{-2} mol) and 2-bromoethanol or iodoethane (2×10^{-2} mol) were first solubilized in 10 mL of acetonitrile, and then the amine solution was added dropwise to the suitable alkyl halide. The mixture was refluxed under an inert atmosphere for 24 h at 70 °C. Subsequently, the solvent was removed by evaporation and the residue was washed three times with acetone. Finally, evaporation at reduced pressure afforded the desired products as colorless solids.

General procedure for the synthesis of the basic organic salts catalysts

The basic organic salts used as catalysts were obtained by anion exchange from the relevant halide salts, employing a reported procedure.[59] To this aim, 15 g of Amberlite IRA-400, Cl^- form was placed inside a column and 10 mL of a 10% (w/V) NaOH aqueous solution was first added with. Then, the resin was washed with ultrapure water, until a neutral eluate was obtained. The suitable halide salt (0.010 mol) was solubilized in methanol–water (70 : 30; v/v) and eluted though the column, collecting the eluate into a flask containing a stoichiometric solution of the suitable acid, in methanol–water (70 : 30; v/v). Then, the resin was eluted with the same solvent until a neutral eluate was obtained. Solvent removal by evaporation afforded the products as solids or viscous oils.

Determination of the Hammett basicity functions of the TSILs

Hammett basicity functions were determined by UV-vis measurements, employing 4-nitrophenol as an indicator. To this aim, the UV-vis spectra of 4-nitrophenol (2×10^{-4} M) in the presence of an equimolar amount of TSIL, in methanol, were recorded. Samples were injected into a quartz cuvette (light path 0.2 cm). The Hammett basicity function (H_-) of each TSILs was calculated using the following equation:

$$H_- = \mathrm{p}K_{\mathrm{ind}} + \log\left(\frac{[\mathrm{I}^-]}{[\mathrm{HI}]}\right) \quad (1)$$

where $\mathrm{p}K_{\mathrm{ind}}$ is the p*K*a value of *p*-nitrophenol in methanol, equal to 11.3, and $[\mathrm{I}^-]$ and [HI] are the concentrations of 4-nitrophenate and 4-nitrophenol, respectively.

The logarithm argument was calculated using the following equation:

$$\frac{[\mathrm{I}^-]}{[\mathrm{HI}]} = \frac{\varepsilon}{\varepsilon_i - \varepsilon} \quad (2)$$

where ε_i is the molar extinction coefficient of *p*-nitrophenate at 388 nm and ε is the is the molar extinction coefficient of *p*-nitrophenol in solution with the TSIL at the same wavelength.

General procedure for the solvolysis of BPA-PC with an ultrasonic probe

In a 25 mL beaker, 2 g of polycarbonate, 2 g of the suitable alcohol, 6 g of 2-methyltetrahydrofuran, and a suitable amount of catalyst were added. The probe tip was placed 0.5 cm under the solution level. The reaction mixture was sonicated under the suitable reaction conditions (temperature, time, ultrasonic power). Then, the unreacted BPA-PC was filtered off, washing the solid with 25 mL of hot methanol. Unreacted BPA-PC was dried and weighed to calculate the conversion. The filtrate, containing BPA and oligomers, was concentrated under reduced pressure. To isolate BPA from the catalyst and oligomers, the residue was added to equal volumes of water and ethyl acetate (25 mL), and the extraction was carried out. The organic phase was then dried on sodium sulfate, filtered, and evaporated under reduced pressure, affording pure BPA.

The conversion and yield were determined according to the following equations:

$$\text{Conversion} = \frac{\text{PC initial mass} - \text{PC residual mass}}{\text{PC initial mass}} \times 100$$

$$\text{Yield} = \frac{\text{Obtained mass of BPA}}{\text{Theoretical mass of BPA}} \times 100$$

General procedure for catalyst recycling

Initially, the reaction under sonochemical conditions and work-up were carried out as already described. The aqueous phase containing oligomers and the catalyst was evaporated under reduced pressure. To the residue obtained, a fresh batch of polycarbonate, methanol, and 2-methyltetrahydrofuran was added. Subsequently, the reaction mixture was sonicated and the work-up procedure was repeated until the values of the conversion and yield were significantly decreased.

Cell cultures and treatments

The hTERT RPE-1 -immortalized retinal pigment epithelial cell was maintained in Dulbecco's modified eagle medium (DMEM) (Gibco, Paisley, UK), supplemented with 10% heat-inactivated fetal bovine serum and 100 U mL^{-1} penicillin and 100 μg mL^{-1} streptomycin. The human mammary epithelial cell line HB2 was grown in the same medium supplemented with hydrocortisone (5 μg mL^{-1}) and insulin (10 μg mL^{-1}). All the culture cells were maintained at 37 °C and 5% CO_2, as already described.[60–62]

For morphological assessment, the cells were seeded on 6-well plates at a density of 5×10^4 cells per well. After 24 h, the cells were treated for 24 h with 1.6 mM of **[TMG][Im]**, **[$C_{222}C_2OHN$][Im]**, and **[C_1C_2OHMor][Im]**. Morphology was observed under a phase-contrast inverted microscope (Carl Zeiss, Oberkochen, Germany) at 200X.

MTT viability assay

The toxic effect of **[TMG][Im]**, **[$C_{222}C_2OHN$][Im]**, and **[C_1C_2-OHMor][Im]** was determined using the MTT assay.[53,54] Cells were plated at 5×10^3 cells per well in 96-well plates and incubated for 24 h before treatment. Stock solutions of DMSO dissolved-**[TMG][Im]**, **[$C_{222}C_2OHN$][Im]**, and **[C_1C_2OHMor][Im]** were diluted to the desired concentrations (25, 50, 100, 200, 400, 800, and 1600 μM) in the culture medium, and added to the wells for a further 48 h incubation. After incubation, 20 μL of 5 mg mL^{-1} of thiazolyl blue tetrazolium bromide (Merck, Darmstadt, Germany) in phosphate buffer saline (PBS) was added to each well in the dark and incubated for a further 2 h at 37 °C.[63]

After removing the medium containing MTT and washing it with PBS three times, 100 μL of DMSO was added to each well to dissolve the formazan.

The absorbance was recorded at 570 nm using a 96-well plate reader (Spark® 20M Tecan Trading AG, Switzerland). The percentage of cell viability compared to the untreated control cells was calculated after subtraction of the blank. The IC_{50}, that is the concentration able to inhibit 50% cell growth, was calculated using a dose-response model, obtained from sigmoidal fitting of the response curves of the percentage inhibition *versus* logarithmic used concentration, using Graph Pad Prism software. Each result was the mean value of three different experiments performed in triplicate.

Data availability

The data supporting this article have been included as part of the ESI.†

Conflicts of interest

There are no conflicts to declare.

Acknowledgements

This study was carried out within the MICS (Made in Italy – Circular and Sustainable) Extended Partnership and received funding from the European Union Next-Generation EU (Piano Nazionale di Ripresa e Resilienza (PNRR) – Missione 4Componente 2, Investimento 1.3 – D.D. 1551.11-10-2022, PE00000004). This manuscript reflects only the authors' views and opinions; neither the European Union nor the European Commission can be considered responsible for them. G.R. thanks PNRR, Missione 4, Componente 1 "Potenziamento dell'offerta dei servizi di istruzione: dagli asili nido all'Università" – Investimento 3.4 "Didattica e competenze universitarie avanzate" e Investimento 4.1 "Estensione del numero di dottorati di ricerca e dottorati innovativi per la pubblica amministrazione e il patrimonio culturale". ^1H and ^{13}C NMR spectra were acquired at ATeN Center of University of Palermo (**https://www.unipa.it/servizi/atencenter/**).

References

1 F. Pinto, P. Costa, I. Gulyurtlu and I. Cabrita, *J. Anal. Appl. Pyrolysis*, 1999, **51**, 39–55.
2 Q. Chen, M. Gundlach, S. Yang, J. Jiang, M. Velki, D. Yin and H. Hollert, *Sci. Total Environ.*, 2017, **584–585**, 1022–1031.
3 L.-J. Feng, X.-D. Sun, F.-P. Zhu, Y. Feng, J.-L. Duan, F. Xiao, X.-Y. Li, Y. Shi, Q. Wang, J.-W. Sun, X.-Y. Liu, J.-Q. Liu, L.-L. Zhou, S.-G. Wang, Z. Ding, H. Tian, T. S. Galloway and X.-Z. Yuan, *Environ. Sci. Technol.*, 2020, **54**, 3386–3394.
4 X. Zhu, H. Wang, B. Liu, D. Yang, F. Liu and X. Song, *Polym. Degrad. Stab.*, 2024, **219**, 110625.
5 T. Su, G.-P. Lu, K. Sun, P. Wu and C. Cai, *J. Environ. Chem. Eng.*, 2023, **11**, 111397.
6 G.-S. Ha, M. Al Mamunur Rashid, J.-M. Ha, C.-J. Yoo, B.-H. Jeon, K. Jeong and K. H. Kim, *Chemosphere*, 2024, **349**, 140781.
7 K. Chan and A. Zinchenko, *J. Cleaner Prod.*, 2023, **433**, 139828.
8 J. T. Bendler, *Handbook of Polycarbonate Science and Technology*, 1st edn, 2000.
9 J. G. Kim, *Polym. Chem.*, 2020, **11**, 4830–4849.
10 J. B. Cyvin, H. Ervik, A. A. Kveberg and C. Hellevik, *Sci. Total Environ.*, 2021, **787**, 147547.
11 Y. Liu and X. Lu, *J. Polym. Sci.*, 2022, **60**, 3256–3268.

12 E. A. Gilbert, M. L. Polo, J. M. Maffi, J. F. Guastavino, S. E. Vaillard and D. A. Estenoz, *J. Polym. Sci.*, 2022, **60**, 3284–3317.
13 X. Song, W. Hu, W. Huang, H. Wang, S. Yan, S. Yu and F. Liu, *Chem. Eng. J.*, 2020, **388**, 124324.
14 C. Alberti, D. Rijono, M. Wehrmeister, E. Cheung and S. Enthaler, *ChemistrySelect*, 2022, **7**, e202104004.
15 J. M. Payne, M. Kamran, M. G. Davidson and M. D. Jones, *ChemSusChem*, 2022, **15**, e202200255.
16 W. Huang, H. Wang, X. Zhu, D. Yang, S. Yu, F. Liu and X. Song, *Appl. Clay Sci.*, 2021, **202**, 105986.
17 J. G. Kim, *Polym. Chem.*, 2020, **11**, 4830–4849.
18 E. Quaranta, A. Dibenedetto, F. Nocito and P. Fini, *J. Hazard. Mater.*, 2021, **403**, 123957.
19 E. Leino, P. Mäki-Arvela, V. Eta, D. Yu. Murzin, T. Salmi and J.-P. Mikkola, *Appl. Catal., A*, 2010, **383**, 1–13.
20 M. A. Pacheco and C. L. Marshall, *Energy Fuels*, 1997, **11**, 2–29.
21 J. Agrell, K. Hasselbo, K. Jansson, S. G. Järås and M. Boutonnet, *Appl. Catal., A*, 2001, **211**, 239–250.
22 L.-C. Hu, A. Oku and E. Yamada, *Polymer*, 1998, **39**, 3841–3845.
23 Y. Zhao, X. Zhang, X. Song and F. Liu, *Catal. Lett.*, 2017, **147**, 2940–2949.
24 E. Quaranta, D. Sgherza and G. Tartaro, *Green Chem.*, 2017, **19**, 5422–5434.
25 Y. Zhao, H. Jiang, S. Xue, M. Liu, F. Liu and S. Yu, *Solid State Sci.*, 2020, **107**, 106317.
26 F. Liu, Y. Xiao, X. Sun, G. Qin, X. Song and Y. Liu, *Chem. Eng. J.*, 2019, **369**, 205–214.
27 M. Liu, J. Guo, Y. Gu, J. Gao, F. Liu and S. Yu, *ACS Sustainable Chem. Eng.*, 2018, **6**, 13114–13121.
28 X. Song, W. Hu, W. Huang, H. Wang, S. Yan, S. Yu and F. Liu, *Chem. Eng. J.*, 2020, **388**, 124324.
29 F. Liu, J. Guo, P. Zhao, M. Jia, M. Liu and J. Gao, *Polym. Degrad. Stab.*, 2019, **169**, 108996.
30 F. Liu, Z. Li, S. Yu, X. Cui and X. Ge, *J. Hazard. Mater.*, 2010, **174**, 872–875.
31 F. Liu, L. Li, S. Yu, Z. Lv and X. Ge, *J. Hazard. Mater.*, 2011, **189**, 249–254.
32 S. Marullo, C. Rizzo, N. T. Dintcheva and F. D'Anna, *ACS Sustain. Chem. Eng.*, 2021, **9**, 15157–15165.
33 F. D'Anna, M. Sbacchi, G. Infurna, N. Tz. Dintcheva and S. Marullo, *Green Chem.*, 2021, **23**, 9957–9967.
34 X. Luo, H. Gong, Z. He, P. Zhang and L. He, *Ultrason. Sonochem.*, 2021, **70**, 105337.
35 M. Singla and N. Sit, *Ultrason. Sonochem.*, 2021, **73**, 105506.
36 Y. Yao, Y. Pan and S. Liu, *Ultrason. Sonochem.*, 2020, **62**, 104722.
37 P. McKeown, M. Kamran, M. G. Davidson, M. D. Jones, L. A. Román-Ramírez and J. Wood, *Green Chem.*, 2020, **22**, 3721–3726.
38 J. Payne and M. D. Jones, *ChemSusChem*, 2021, **14**, 4041–4070.
39 A. C. Fernandes, *Green Chem.*, 2021, **23**, 7330–7360.
40 S. P. F. Costa, A. M. O. Azevedo, P. C. A. G. Pinto and M. L. M. F. S. Saraiva, *ChemSusChem*, 2017, **10**, 2321–2347.
41 C. R. McElroy, A. Constantinou, L. C. Jones, L. Summerton and J. H. Clark, *Green Chem.*, 2015, **17**, 3111–3121.
42 S.-P. Chen, J.-L. Zhu, X.-R. Chen, Z.-H. Wang, Y.-J. Dan, J. Wang, S.-Y. Zhou, G.-J. Zhong, H.-D. Huang and Z.-M. Li, *Green Chem.*, 2023, **25**, 9322–9334.
43 M. T. Donato, J. Deuermeier, R. Colaço, L. C. Branco and B. Saramago, *Molecules*, 2023, **28**, 2678.
44 K. Alorku, C. Shen, Y. Li, Y. Xu, C. Wang and Q. Liu, *Green Chem.*, 2022, **24**, 4201–4236.
45 F. D'Anna and R. Noto, *Tetrahedron*, 2007, **63**, 11681–11685.
46 F. D'Anna, P. Vitale and R. Noto, *J. Org. Chem.*, 2009, **74**(16), 6224–6230.
47 C. Rizzo, F. D'Anna, S. Marullo and R. Noto, *J. Org. Chem.*, 2009, **74**, 6224–6230.
48 C. Rizzo, F. D'Anna and R. Noto, *RSC Adv.*, 2016, **6**, 58477–58483.
49 A. D. Headley and N. M. Jackson, *J. Phys. Org. Chem.*, 2002, **15**, 52–55.
50 J. Dupont and J. Spencer, *Angew. Chem., Int. Ed.*, 2004, **43**, 5296–5297.
51 S. Huang, B. Yan, S. Wang and X. Ma, *Chem. Soc. Rev.*, 2015, **44**, 3079–3116.
52 S. A. Cucinell and E. Arsenal, *Arch. Environ. Health*, 1974, **28**, 272–275.
53 F.-S. Liu, Z. Li, S.-T. Yu, X. Cui, C.-X. Xie and X.-P. Ge, *J. Polym. Environ.*, 2009, **17**, 208–211.
54 C. S. Bhogle and A. B. Pandit, *Ultrason. Sonochem.*, 2019, **58**, 104667.
55 X. Song, W. Hu, W. Huang, H. Wang, S. Yan, S. Yu and F. Liu, *Chem. Eng. J.*, 2020, **388**, 124324.
56 F. Liu, R. Ping, P. Zhao, Y. Gu, J. Gao and M. Liu, *ACS Sustainable Chem. Eng.*, 2019, **7**, 13517–13522.
57 V. Ramkumar and R. L. Gardas, *J. Mol. Liq.*, 2021, **343**, 117664.
58 W. Lee, J.-Y. Shin, J.-H. Cha, K.-S. Kim and S.-P. Kang, *J. Ind. Eng. Chem.*, 2016, **38**, 211–216.
59 I. Dinarès, C. Garcia de Miguel, A. Ibáñez, N. Mesquida and E. Alcalde, *Green Chem.*, 2009, **11**, 1507.
60 G. Schiera, C. M. Di Liegro, V. Puleo, O. Colletta, A. Fricano, P. Cancemi, G. Di Cara and I. Di Liegro, *Int. J. Oncol.*, 2016, **49**, 1807–1814.
61 R. Musso, G. Di Cara, N. N. Albanese, M. R. Marabeti, P. Cancemi, D. Martini, E. Orsini, C. Giordano and I. Pucci-Minafra, *J. Proteom.*, 2013, **90**, 115–125.
62 I. Pucci-Minafra, N. N. Albanese, G. Di Cara, L. Minafra, M. R. Marabeti and P. Cancemi, *Connect. Tissue Res.*, 2008, **49**, 252–256.
63 M. Massaro, G. Barone, V. Barra, P. Cancemi, A. Di Leonardo, G. Grossi, F. Lo Celso, S. Schenone, C. Viseras Iborra and S. Riela, *Int. J. Pharm.*, 2021, **599**, 120281.